Electrochemical Annealing and its Relevance in Metal Electroplating: An Atomistic View

Ernesto Pichardo-Pedrero, Guillermo L. Beltramo and Margret Giesen*

Institute for Bio- and Nanosystems, IBN 4 Biomechanics, Forschungszentrum Jülich, D 52425 Jülich, Germany

Abstract

Using electrochemical scanning tunneling microscopy we have studied the decay of monolayer high islands on Au(001) electrodes as a function of electrode potential and as a function of the specifically adsorbed ion on the surface. We find that island decay is diffusion limited and transport rates depend strongly on electrode potential and on the specifically adsorbed ion, an effect qualitatively known for long now. In this study we quantitatively investigate the transport rates and find values for the relevant transport energy barriers in the different electrolytes.

* To whom all correspondence should be addressed: m.giesen@fz-juelich.de; http://www.fz-juelich.de/isg/index.php?index=225; Phone: +49 2461 614108; Fax: +49 2461 613907

1. Introduction

With the ever more shrinking dimensions of surface nanostructures which are expected to lead further down the road of device minimization, modern device structures and printed circuits are approaching the nm-scale. Hence, the question whether the nanostructures are stable on the atomic scale for the life-time of storage devices becomes relevant. For quite a number of years, solid surfaces and in particular surface structures such as steps were considered merely as static objects [1]. Throughout the 90ies, however, it became obvious that surface atoms and defects are very mobile and the mobility may considerably determine the physical and chemical characteristics of solid surfaces and their interaction with environment [2, 3]. In order to understand the mobility of atoms and defects theoretical methods from statistical thermodynamics set out to conquer surface science studies and the analysis of atom and defect migration. Simultaneously, modern enhanced computer capacity enabled to calculate the relevant migration energies using ab initio calculations such as density functional theory [4]. Simulations of surface diffusion processes [2] had also their input into these research studies.

Whereas atom migration on solid surfaces in contact with vacuum or a gas phase is quite well understood today, technically more relevant systems such as solid surfaces in electrochemical environment still pose a challenge to experiment as well as to theory. The reason lies in the presence of the liquid, the ions contained in the electrolyte and their interaction with the solid via direct chemical interactions, adsorption phenomena and charge transfer between the solid and the liquid. To date there is only few people who dedicated their scientific focus to atom migration at the solid liquid interface and to the quantitative analysis and the understanding of diffusion processes on solid surfaces in contact with a liquid [3, 5-16]. In particular the theoretical input of the Harald Ibach - to whom this volume is dedicated - and his effort to achieve a thorough insight to atom migration at the solid/liquid interface led to quite some break-ups of common believes and opened new pathways to the understanding of solid/liquid interfaces. For our group of experimentalists who experienced the pleasure and challenge to

closely and fruitfully collaborate with him for quite a number of years it is a particular honor to present some of our most recent activities on scanning tunneling microscopy studies on atom migration on gold electrodes - a topic he dedicated his main interest throughout the last decade of his scientific work.

2. A brief review

Quantitative studies on atomic motion on metal surfaces in electrolyte were triggered by an observation of the Kolb group in Ulm when they discovered that steps on silver electrodes appear frizzy [17]. The same phenomenon was described earlier by our group for steps on silver surfaces in ultra-high vacuum (UHV) [18] and is due to fast atom diffusion along the silver steps during the comparably slow scanning process of the scanning tunneling microscope (STM) [19]. In a fruitful collaboration with the Kolb group we later analyzed the step fluctuations on silver electrodes in contact with an electrolyte as a function of the electrode potential [20] and opened a gateway to a new understanding of surface migration on electrode surfaces. More recently we extended the previous data on silver surfaces to measurements of the activation barrier by introducing temperature-variable STM investigations of electrode surfaces in liquid environment [21, 22]. Whereas our temperature-variable approach to surface diffusion phenomena on electrodes were the first data of that kind, it was only six years later that another group attacked the challenge of measuring activation energies in electrolyte environment of adsorbate diffusion on Cu(100) in HCl solution [13].

For step fluctuations [20, 23, 24] as well as for island decay studies [14, 25] a general observation was made that the mobility on electrode surfaces increases exponentially with electrode potential. The exponential increase of the transport rates with electrode potential has an important technical relevance in electroplating processes of metal surfaces: It is well-known fact that raising the electrode potential is equivalent to raising the temperature. To

emphasize this analogy the term "electrochemical annealing" was created for this phenomenon [26-29]. Though qualitatively well-known for almost two decades now the explanation for the exponential increase of the transport rates with potential was given only recently by our group [25]: We showed that the common cause rests in the thermodynamic condition of charged electrolyte surfaces held at constant potential. We argued that because of this thermodynamic constraint, all formation energies and activation energies are renormalized by an electrostatic energy term arising from the interaction of dipole moment of the defect with the electric field at the interface. This interpretation was recently adopted by Magnussen and coworkers to explain experimental data on adsorbate diffusion on Cu(100) in HCl solution [13].

A further effect which is known from electroplating of metal surfaces is that some additives to the electrolyte may enhance transport rates while keeping the electrode potential constant. To emphasize the result that metals appear shinier when those additives were used, these substances were called "brightener". They increase transport rates such that defects are healed out faster and the residual surface roughness becomes smaller.

After this brief review we will present new data on the decay of Au islands on Au(001) electrodes in chloride containing electrolytes. In contrast to previous data obtained in sulfuric acid [25, 30-32], the island decay is now controlled by chloride ions in the electrolyte. We will consider the potential dependence of the island decay rates and by comparison with the previous data on Au(001) electrodes in sulfuric acid solution we obtain information on the dependence of the rates on the active anion in the solution.

3. Experimental set-up

The measurements were performed with the electrochemical version of the Topometrix TMX 2010 Discoverer STM. Our instrument was modified to enable temperature variable STM recording with high thermal drift stability and is described in detail elsewhere [21, 22]. In the

studies reported here, however, all experimental results were obtained at 297 K. The tip and the sample potential are independently controlled via a bipotentiostat.

Our studies on the island shape were performed on Au(100) single crystal electrodes which were cut by spark erosion from a single crystal rod, oriented by diffractometry and polished to the desired orientation within 0.1°, which is the accuracy of high-quality single crystals. The accuracy is naturally limited by the mosaic structure of the crystal. Prior to experiment, the Au(100) electrode was heated in a hydrogen atmosphere and then flame annealed for about 5 min to about 900°C. The temperature was visually controlled by the color of the annealed crystal. After thoroughly rinsing the cell with Milli-Q water, the crystal was mounted in the electrochemical STM cell which was connected to the bipotentiostat. The crystal surface was then brought in contact with the electrolyte under potential control. This was visually checked at the beginning of each STM experiment by the presence of the well-ordered quasi-hexagonal reconstruction of the clean Au(100) surface [33]. The mean terrace width of the crystal was of the order of 100 nm. As an electrolyte, we used suprapure $HClO_4$ and HCl (Merck) and as described in previous papers suprapure H_2SO_4 as well as Milli-Q water from a Millipore Elix 3 and A10 Gradient system (18.2 MΩ cm^{-1}; organic contents <3 ppb). The STM measurements were performed in 100 mM $HClO_4$ + 1mM HCl and 50 mM H_2SO_4.

The tunneling tips used in the experiments were etched from polycrystalline tungsten wires and coated with polyethylene to avoid Faraday currents at the foremost part of the tip [34]. We used a tunneling current of 2 nA. The typical time per image was about 60 s and the STM images were recorded with a 400×400 pixel resolution in the constant current mode. High-purity, flame-annealed Pt wires (Goodfellow, 99.999%) served as counter and quasi-reference electrodes. In the following, the electrode potentials of the metal sample are, however, given with respect to the saturated calomel electrode (SCE). As a caveat we emphasize that the electrode potentials denoted here are the nominal values given by the bipotentiostat.

After each experiment we checked the potential by measuring a cyclic voltamogram in the STM cell. Still we cannot exclude that the potential values as denoted here might deviate from the real potential by about 50 mV due to possible shifts in the potential during experiment. For the experimental analysis the monatomic high Au islands were created by stepping the electrode potential from where the crystal was immersed in the electrolyte to higher potentials where the (hex)-surface reconstruction is lifted [33]. Fig. 1 shows cyclic voltamograms of Au(001) in 10 mM $HClO_4$ + 1 mM HCl (dashed black curve) and in 5 mM H_2SO_4 (solid grey curve) similar to those electrolytes as used in the STM measurements. The voltamograms were obtained in a separate electrochemical cell and were measured against a saturated calomel electrode (SCE). The peaks around 140 and 370 mV, respectively, are related to the lifting of the quasi-hex reconstruction of the Au(001) electrode in the two electrolytes.

The STM experiments were performed at electrode potentials between +300 and +700 mV vs. SCE in the case of Au(001) in 50 mM H_2SO_4 and between +190 and +450 mV in the case of Au(001) in 100 mM $HClO_4$ + 1 mM HCl. The island shapes of individual islands in the STM images are determined by a special computer code which searches for the maximum slope in the grey scale in an STM image described in more detail elsewhere [30, 32]. Starting at a distinct point in the centre of an island, the program finds the radius of an island for a given polar angle. The accuracy of the overall shape is given by the step width between individual polar angles which can be chosen to be a minimum value of 1° (in other words by the number of base points, at maximum 360), by the pixel noise and by the noise in the STM image. In the experiments reported here, the island shapes were determined using 200 base points (i.e. 200 number pairs consisting of the island radius and the corresponding polar angle) in the case of Au(001) in 50 mM H_2SO_4 and using 360 base points in the case of Au(001) in 100 mM $HClO_4$ + 1 mM HCl. Depending on the chosen electrode potential, good experimental conditions lasted 30 min to 2 h. Then, generally, contamination of the electrolyte in the open STM cell became visible and the measurements were terminated.

4. Results

Fig. 2 shows representative STM image sequences of Au islands on Au(100) in (a) 50 mM H_2SO_4 at +400 mV vs. SCE and (b) 100 mM $HClO_4$ + 1 mM HCl at +400 mV SCE. The islands are mobile due to atomic motion at the island edges. Smaller islands vanish and larger islands grow, a phenomenon known as Ostwald ripening [35-37]. Coalescence events where islands merge with steps or with other islands are also observed. The quantitative analysis of such events, however, will be discussed elsewhere [38]. Here, we will discuss exclusively island decay events.

In Ostwald theory two basic scenario are distinguished (for a recent review see [3]): In the first, the time-limiting step of the island decay is the detachment/re-attachment of atoms at the island edge. Then, the island area is a linear function of time. In the second case, the time-limiting step is the diffusion of atoms on the terrace, then the island area changes according to $t^{2/3}$. In experiment, substantial deviations from the exponent 2/3 may be found. This is due to the limit of basic approximations made in the analytical theory [3]. However, in the diffusion-limited case, the decay curves are always curved. A further typical observation in the diffusion-limited case is the fact that decay curves of individual islands are influenced by their neighborhood [39, 40]: Larger islands in the vicinity of small islands initially grow in size due to the mass gain during the decay of their smaller neighbors.

As becomes obvious from Fig. 3, the decay curves of islands on Au(001) are curved. Furthermore, large islands may initially grow in size (see Fig. 3(b)). Hence, the island decay is diffusion limited. We have measured the island decay on Au(001) in 50 mM H_2SO_4 [32] and in 100 mM $HClO_4$ + 1 mM HCl in the potential ranges between +300 and +700 mV vs. SCE and +190 and +450 mV, respectively. For all potentials and electrolytes the island decay is diffusion limited.

In order to investigate the influence of the electrode potential and the specifically adsorbed anion on the decay rate, we have determined the rate of individual decay curves for a specific island size A_0 = 100 Ω (with Ω=0.0832 nm^2 being the area of an atom on Au(001)). In Fig. 4, the results are plotted as black circles (100 mM $HClO_4$ + 1 mM HCl) and grey squares (50 mM H_2SO_4 [25]).

The solid lines are exponential fits to the data. For a given potential, the island decay rates are higher for the case of chloride adsorption on Au(001) compared to the case of sulfate adsorption. In both cases, the data can be fitted by an exponential increase in agreement with our previous report [25].

5. Discussion

As was discussed in detail in [25] all formation energies and activation energies are renormalized by an electrostatic energy term arising from the interaction of the dipole moment of the defect with the electric field at the charged electrolyte interface held at constant potential. To first order, formation and activation energies E are therefore a linear function of the electrode potential ϕ,

$$E(\phi) = E(0) - \lambda e \phi , \qquad (1)$$

with e the electron charge and λ a factor depending on the dipole moment of the defect considered. We note that λ may become negative. Without restriction of generality we write the electrode potential with respect to the potential ϕ=0. Whereas in ref. [25] eq. (1) was analytically derived from thermodynamical considerations, the same ansatz was empirically derived already several years ago [20]. In the previous work, however, merely plausibility arguments could be given to justify the use of eq. (1). The linear relationship between energy

and electrode potential, however, was then successfully used to derive an estimate for the relevant activation and formation energies from the exponential dependence of step fluctuations on the potential [3, 20-23, 41, 42]. Here, we would like to perform a similar analysis for the exponential increase of the island decay rates with electrode potential: For diffusion limited island decay on a square lattice substrate[1], the decay rate of the island area A is given by [3]

$$\frac{\mathrm{d}A}{\mathrm{d}t} \approx -\frac{4\sqrt{\pi}\nu_0\Omega}{\ln\left(\frac{r_\mathrm{o}}{r_\mathrm{i}}\right)} \exp\left(-\frac{E_\mathrm{ad}(\phi)+E_\mathrm{diff}(\phi)}{k_\mathrm{B}T}\right) \frac{\beta\Omega}{k_\mathrm{B}T}\left(\frac{1}{r_\mathrm{i}}-\frac{1}{r_\mathrm{o}}\right). \qquad (2)$$

The pre-exponential factor ν_0 is assumed to be independent of the potential ϕ and to be of the typical order $\nu_0 = 10^{13}\mathrm{s}^{-1}$ [44]. Ω=0.0832 nm² is the area of an atom on the Au(001) surface and β is the potential dependent step line tension. For Au(001) in 100 mM $HClO_4$ + 1 mM HCl, β is merely a weak function of ϕ and is of the order $\beta(\phi) \approx \text{const.} = 28\,\mathrm{meV}/a_{||}$ [38], with $a_{||}$ = 0.288 nm the nearest neighbor atomic distance on Au(001). For Au(001) in 50 mM H_2SO_4, β shows a stronger potential dependence [30, 31], however, for our purposes here, a mean value of $\beta(\phi) \approx \text{const.} = 40\,\mathrm{meV}/a_{||}$ is still a good approximation.

In Ostwald theory, the decaying adatom island with radius r_i ("inner" island radius) is considered to be located within a larger vacancy island with radius r_o ("outer" island radius). Those radii occur in the decay equation (2). In real experiments, this ideal situation is rarely achieved. Rather, islands of the same kind (adatom or vacancy islands) are located next to each other and in order to obtain a full description of the experimentally observed decay curves, the Laplace equations for surface diffusion must be solved for the total island

[1] In the decay equation a factor η must be considered which is η=2/√π for a square lattice [43] G. Schulze Icking-Konert, M. Giesen and H. Ibach, Surf. Sci. 398 (1998) 37-48.

ensemble [39, 45, 46]. In most cases, however, a reasonable approximation is made if one assumes the inner radius r_i to be the radius of the decaying island considered and the outer radius r_o to be the mean distance of neighboring islands [25]. For our purposes here reasonable values are $r_o/r_i \approx 2$ and $r_i \approx 10\, a_{\|}$.

According to eq. (1), the adatom formation energy E_{ad} from a kink site in the island edge onto the terrace and the diffusion barrier E_{diff} on the terrace are potential dependent and given by

$$E_{ad}(\phi) + E_{diff}(\phi) = E_{ad}(0) + E_{diff}(0) - e\lambda\phi\,. \tag{3}$$

Using eq. (3) in (2) we obtain

$$\frac{dA}{dt} \approx -\frac{4\sqrt{\pi}\nu_0\Omega}{\ln\left(\frac{r_o}{r_i}\right)} \exp\left(-\frac{E_{ad}(0)+E_{diff}(0)}{k_B T}\right)\exp\left(\frac{\lambda e\phi}{k_B T}\right)\frac{\beta\Omega}{k_B T}\left(\frac{1}{r_i}-\frac{1}{r_o}\right) \tag{4}$$

Using the values for Ω, ν_0, β, r_i and r_0 as discussed above we find

(i) for Au(001) in 100 mM $HClO_4$ + 1 mM HCl

$$\dot{A}(\phi) \approx -5.63\cdot 10^{13}\,\Omega\,\mathrm{s}^{-1}\,\exp\left(-\frac{E_{ad}(0)+E_{diff}(0)}{k_B T}\right)\exp\left(\frac{\lambda e\phi}{k_B T}\right) \tag{5}$$

and

(ii) for Au(001) in 50 mM H_2SO_4

$$\dot{A}(\phi) \approx -8.04\cdot 10^{13}\,\Omega\,\mathrm{s}^{-1}\,\exp\left(-\frac{E_{ad}(0)+E_{diff}(0)}{k_B T}\right)\exp\left(\frac{\lambda e\phi}{k_B T}\right) \tag{6}$$

Fitting eqs. (5), (6) to the experimental data in Fig. 4 one gets

(i) for Au(001) in 100 mM $HClO_4$ + 1 mM HCl

$$\lambda = 0.34 \pm 0.03 \quad \textit{and} \quad E_{\mathrm{ad}}(0) + E_{\mathrm{diff}}(0) \approx 0.9\,\mathrm{eV} \tag{7}$$

and

(ii) for Au(001) in 50 mM H_2SO_4

$$\lambda = 0.42 \pm 0.03 \quad \textit{and} \quad E_{\mathrm{ad}}(0) + E_{\mathrm{diff}}(0) \approx 1.1\ \mathrm{eV}\ . \tag{8}$$

We emphasize that E_{ad} and E_{diff} are potential dependent and hence, the values in eqs. (7), (8) are valid exclusively for the chosen reference potential at 0 V. However, by using eq. (3) one easily calculates the respective values for any given potential (Fig. 5). The variation of E_{ad}+E_{diff} is of the order of 30 % over the considered potential range. The error margins of the experimental values at 0 V are of the order of 10-20 %. Hence, it is reasonable to discuss the results for E_{ad}+E_{diff} in the view of an almost constant energy value over the whole potential range. For both electrolytes, the energy value is of the order of 1 eV. One can safely say, however, that the energy value for the chloride controlled electrolyte is systematically smaller than the energy for the sulfate containing solution. This is in agreement with the general understanding that chloride serves as a brightener in metal plating, i.e. enhances surface mass transport and decreases relevant transport energy barriers.

If one compares our results with other data on E_{ad}+E_{diff} , one finds that the values obtained here are in the right order of magnitude: Theoretical values on E_{ad}+E_{diff} for Au(001) in electrolyte or respective experimental data are not available to the best of our knowledge. One may compare the values, however, with previous results for Cu(111) in 1 mM HCl where

$E_{ad}+E_{diff}$ = 0.60±0.12 eV at ϕ = –420 mV SCE was found [22, 42]. Respective experimental data for metal surfaces in ultra-high vacuum (UHV) are available for Cu(111) ($E_{ad}+E_{diff}$ = 0.76 ± 0.04 eV [43]), Ag(111) ($E_{ad}+E_{diff}$ = 0.71 ± 0.03 eV [47]) and Cu(001) ($E_{vac}+E_{diff}$ = 0.73 ± 0.12 eV - here mono-vacancies are the dominant transport species rather than single adatoms - [40, 48, 49]). Theoretical data for metal (001) surfaces under vacuum conditions were calculated e.g. for Ni(001) where $E_{ad}+E_{diff}$ was found to be of the order of 1 to 1.7 eV if adatoms were considered to be the transport species [50-52]. For Cu(001) and Ag(001) merely adatom diffusion was considered and values of $E_{ad}+E_{diff}$ between 0.83 and 0.93 eV [52, 53], respectively between 0.58 and 1.21 eV [50, 52, 54] were obtained.

According to [25] the factor λ is related to the dipole moment of the defect. With $E=E_{ad}+E_{diff}$ one has:

$$E(\phi) = E(0) - \Delta E = E(0) - \frac{\mu^+ - \mu_0}{\varepsilon_0}\sigma(\phi) \qquad (9)$$

Here, μ^+ is the dipole moment of the defect in an activated transition state and μ_0 is the dipole moment in the ground state. For the creation of an adatom from a kink site to a terrace site, μ^+ is the dipole moment of the adatom on a four-fold hollow terrace site and μ_0 is the dipole moment of the kink. The kink, however, does not vanish after creation of the adatom on the terrace but leaves a new kink site shifted by one atom distance. For a diffusing atom on the terrace μ^+ is to be identified as the dipole moment of an adatom in a transition bridge state, $\mu^+ \equiv \mu_{ad}^+$, and μ_0 is again the dipole moment of the adatom in the four-fold hollow terrace site. Hence, E can be written as

$$E(\phi) = E(0) - \frac{\mu_{ad}^{+}}{\varepsilon_0}\sigma(\phi). \qquad (10)$$

with $\Delta E = \frac{\mu_{ad}^{+}}{\varepsilon_0}\sigma(\phi)$.

Eq. (10) can be compared with eq. (3), in which ΔE is to be written as $\Delta E = e\lambda\phi$. The result is shown in Fig. 6. For the calculation of eq. (10) in Fig. 6 we have used $\mu_{ad}^{+} = 0.144\ e$ Å as obtained from cluster calculations for an adatom on a Au(001) surface with no liquid present [25]. This value should be in the right order of magnitude [55]. $\sigma(\phi)$ has been measured for 50 mM H_2SO_4 and 10 mM $HClO_4$ + 1 mM HCl and will be published elsewhere [55].

Good agreement between eq. (3) and (10) is achieved exclusively for small potentials. According to [25] the linear approximation in eq. (10) is strictly valid only when there is no specific adsorption on the electrode. In both electrolytes, however, sulfate respectively chloride ions are specifically adsorbed on the gold surface, in particular for electrode potentials larger than the potential of zero charge (pzc). Hence, one would indeed not expect a good agreement between the curves for positive potentials with respect to pzc.

Summary

In summary we have analyzed the decay of monatomic high gold islands on Au(001) electrodes in sulfate and chloride dominated electrolytes. We find that island decay on Au(001) metal electrodes in these electrolytes is supported by single adatom diffusion and the decay is diffusion limited. The island decay rate increases exponentially with electrode potential. From a detailed atomistic analysis of the potential dependence we obtain reasonable estimates for the sum of the adatom formation energy E_{ad} and the surface diffusion barrier

E_{diff} (E_{ad}+E_{diff} ≈ 1.1 eV in 50 mM H_2SO_4 and E_{ad}+E_{diff} ≈ 0.9 eV in 100 mM $HClO_4$ + 1 mM HCl).

Acknowledgement

Throughout the years M.G. had the pleasure to work with Harald on the topic of atom migration on solid surfaces and quite a number of students, PostDocs and collaborators had contributed to our work. At this place, M.G. would like to take the opportunity to express her deep thanks to all of them:

Sascha Baier, Guillermo Beltramo, Sabine Dieluweit, Michael Dietterle, Ted L. Einstein, Josef Frohn, James B. Hannon, Georg Schulze Icking-Konert, Julian Ikonomov, Rainer Jentjens, Christian Klünker, Dieter M. Kolb, Udo Linke, Jorge E. Müller, Ernesto Pichardo Pedrero, Matthias Poensgen, Rudolf Randler, Wolfgang Schmickler, Frank Schmitz, Dietmar Stapel, Christoph Steimer, Kirilka Starbova, J. Francis Wolf.

Furthermore, financial support was given by the Deutsche Forschungsgemeinschaft and the Fonds der Chemischen Industrie.

References

[1] G.A. Somorjai, R.W. Joyner and B. Lang, Proceedings of the Royal Society of London, Series A (Mathematical and Physical Sciences) 331 (1972) 335-46.

[2] H.-C. Jeong and E.D. Williams, Surf. Sci. Rep. 34 (1999) 171.

[3] M. Giesen, Prog. Surf. Sci. 68 (2001) 1.

[4] W. Kohn and L.J. Sham, Phys. Rev. 140 (1965) A1133.

[5] O.M. Magnussen and M.R. Vogt, Phys. Rev. Lett. 84 (2000) 357.

[6] P. Broekmann, M. Wilms, M. Kruft, C. Stuhlmann and K. Wandelt, J. Electroanal. Chem. 467 (1999) 307.

[7] Y. He and E. Borguet, J. Phys. Chem. B 105 (2001) 3981.

[8] W. Schmickler and U. Stimming, J. Electroanal. Chem. 366 (1994) 203.

[9] H. Ibach, M. Giesen and W. Schmickler, J. Electroanal. Chem. 544 (2003) 13-23.

[10] M. Del Popolo, Surf. Sci. 597 (2005) 133-155.

[11] M.G.D. Pópolo, E.P.M. Leiva and W. Schmickler, Angewandte Chemie International Edition 40 (2001) 4674-4676.

[12] O. Magnussen, Faraday discussions of the Chemical Society 121 (2002) 43-52.

[13] T. Tansel and O.M. Magnussen, Phys. Rev. Lett. 96 (2006) 026101.

[14] N. Hirai, K. Watanabe and S. Hara, Surf. Sci. 493 (2001) 568.

[15] N. Hirai, K. Watenabe, A. Shiraki and S. Hara, J. Vac. Sci. Technol. B 18 (2000) 7.

[16] N. Hirai, H. Tanaka and S. Hara, Applied Surface Science 130-132 (1998) 506.

[17] M. Dietterle, T. Will and D.M. Kolb, Surf. Sci. 327 (1995) L495.

[18] J.F. Wolf, B. Vicenzi and H. Ibach, Surf. Sci. 249 (1991) 233.

[19] M. Poensgen, J.F. Wolf, J. Frohn, M. Giesen and H. Ibach, Surface Science 274 (1992) 430.

[20] M. Giesen, M. Dietterle, D. Stapel, H. Ibach and D.M. Kolb, Surf. Sci. 384 (1997) 168.

[21] S. Baier and M. Giesen, Phys. Chem. Chem. Phys. 2 (2000) 3675.

[22] M. Giesen and S. Baier, J. Phys. Condens. Matter 13 (2001) 5009.

[23] M. Giesen, R. Randler, S. Baier, H. Ibach and D.M. Kolb, Electrochim. Acta 45 (1999) 527.

[24] M. Giesen and D.M. Kolb, Surf. Sci. 468 (2000) 149-164.

[25] M. Giesen, G. Beltramo, S. Dieluweit, J. Muller, H. Ibach and W. Schmickler, Surf. Sci. 595 (2005) 127-137.

[26] G.J. Cali, G.M. Berry, M.E. Bothwell and M.P. Soriaga, J. Electroanal. Chem. 297 (1991) 523.

[27] A.S. Dakkouri, Solid State Ionics 94 (1997) 99.

[28] L.B. Goetting, B.M. Huang, T.E. Lister and J.L. Stickney, Electrochim. Acta 40 (1995) 143.

[29] J.L. Stickney, I. Villegas and C.B. Ehlers, J. Am. Chem. Soc. 111 (1989) 6473.

[30] S. Dieluweit, H. Ibach and M. Giesen, Faraday Discuss. 121 (2002) 27.

[31] S. Dieluweit and M. Giesen, J. Electroanal. Chem. 524-525 (2002) 194.

[32] S. Dieluweit and M. Giesen, J. Phys. Condens. Matter 14 (2002) 4211.

[33] D.M. Kolb, Progress in Surface Science 51 (1996) 109.

[34] C.E. Bach, R.J. Nichols, W. Beckmann, H. Meyer, A. Schulte, J.O. Besenhard and P.D. Jannakoudakis, J. Electrochem. Soc. 140 (1993) 2181.

[35] L.M. Lifshitz and V.V. Slyozov, J. Phys. Chem. Solids 19 (1961) 35.

[36] C. Wagner, Z. Elektrochem. 65 (1961) 581.

[37] P. Wynblatt and N.A. Gjostein, in *Progress in Solid State Chemistry*, J.O. McCaldin and G. Somorjai, Editors, (1975), Pergamon Press, Oxford, p. 21.

[38] E. Pichardo-Pedrero and M. Giesen, Electrochim. Acta in press, doi:10.1016/j.electacta.2006.10.061 (2006).

[39] W. Theis, N.C. Bartelt and R.M. Tromp, Phys. Rev. Lett. 75 (1995) 3328.

[40] J.B. Hannon, C. Klünker, M. Giesen, H. Ibach, N.C. Bartelt and J.C. Hamilton, Phys. Rev. Lett. 79 (1997) 2506-2509.

[41] M. Giesen and D.M. Kolb, Surf. Sci. 468 (2000) 149.

[42] S. Baier, S. Dieluweit and M. Giesen, Surf. Sci. 502-503 (2002) 463-473.

[43] G. Schulze Icking-Konert, M. Giesen and H. Ibach, Surf. Sci. 398 (1998) 37-48.

[44] G.L. Kellogg, Surf. Sci. Rep. 21 (1994) 1.

[45] G.S. Icking-Konert, M. Giesen and H. Ibach, Surf. Sci. 398 (1998) 37.

[46] G. Rosenfeld, K. Morgenstern, I. Beckmann, W. Wulfhekel, E. Laegsgaard, F. Besenbacher and G. Comsa, Surf. Sci. 402-404 (1998) 401.

[47] K. Morgenstern, G. Rosenfeld and G. Comsa, Phys. Rev. Lett. 76 (1996) 2113.

[48] C. Klünker, J.B. Hannon, M. Giesen, H. Ibach, G. Boisvert and L.J. Lewis, Phys. Rev. B 58 (1998) R7556.

[49] J. Ikonomov, K. Starbova and M. Giesen, Surf. Sci. in press (2007) doi:10.1016/j.susc.2007.01.004.

[50] J. Merikoski, I. Vattulainen, J. Heinonen and T. Ala-Nissila, Surf. Sci. 387 (1997) 167.

[51] P. Stoltze, J. Phys. Condens. Matter 6 (1994) 9495.

[52] H. Mehl, O. Biham, I. Furman and M. Karimi, Phys. Rev. B60 (1999) 2106.

[53] M. Karimi, T. Tomkowski, G. Vidali and O. Biham, Phys. Rev. B52 (1995) 5364.

[54] B.D. Yu and M. Scheffler, Phys. Rev. B55 (1997) 13916.

[55] G. Beltramo, H. Ibach and M. Giesen, Surf. Sci. in press (2007).

Figure Captions

Fig. 1: Cyclic voltamograms of Au(001) in 10 mM $HClO_4$ + 1 mM HCl (dashed black curve) and 5 mM H_2SO_4 (solid grey curve). Scanrate 10 mV/s.

Fig. 2: STM image sequences of Au(001) electrodes in (a) 50 mM H_2SO_4 and (b) 100 mM $HClO_4$ + 1 mM HCl.

Fig. 3: Decay curves of Au islands on Au(001) in (a) 50 mM H_2SO_4 at +500 mV SCE [32] and (b) 100 mM $HClO_4$ + 1 mM HCl at +190 mV SCE. The island area is given in atoms (the area of an atom is Ω=0.0832 nm^2).

Fig. 4: Decay rate of Au islands on Au(001) in 50 mM H_2SO_4 (grey squares) [25] and 100 mM $HClO_4$ + 1 mM HCl (black circles). The decay rate was determined for islands of size A_0=100 Ω.

Fig. 5: Potential dependence of E_{ad}+$E_{diff\ f}$ for Au(001) in 50 mM H_2SO_4 (grey line) and 100 mM $HClO_4$ + 1 mM HCl (black line) according to eqs. (3), (7) and (8) using a potential-independent pre-exponential factor of ν_0=10^{13} s^{-1}.

Fig. 6: Plot of $\Delta E = \frac{\mu_{ad}^{+}}{\varepsilon_0}\sigma(\phi)$ calculated from the dipole moment μ_{ad}^{+} of an adatom on the surface and from the measured surface charge $\sigma(\phi)$ according to eq. (10) for Au(001) in 50 mM H_2SO_4 (grey solid line) and in 10 mM $HClO_4$ + 1 mM HCl (black solid line) [55]. The dashed lines are the results for $\Delta E = e\lambda\phi$ using eqs. (7), (8). For the two electrolytes the position of the pzc is indicated by the vertical dotted lines at –0.015 and –0.12 V, respectively. See text for discussion.

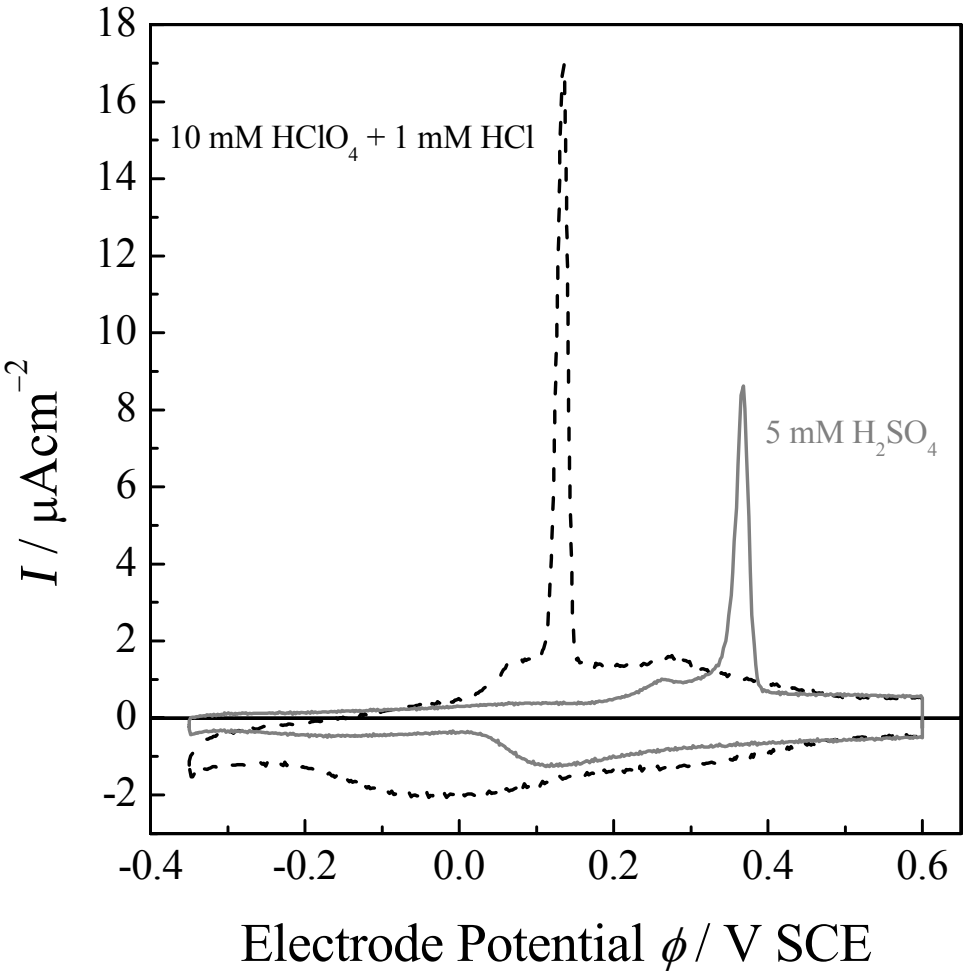
10 mM HClO4 + 1 mM HCl
5 mM H2SO4
I / μAcm−2
Electrode Potential ϕ / V SCE
18
16
14
12
10
8
6
4
2
0
-2
-0.4
-0.2
0.0
0.2
0.4
0.6

Fig. 1

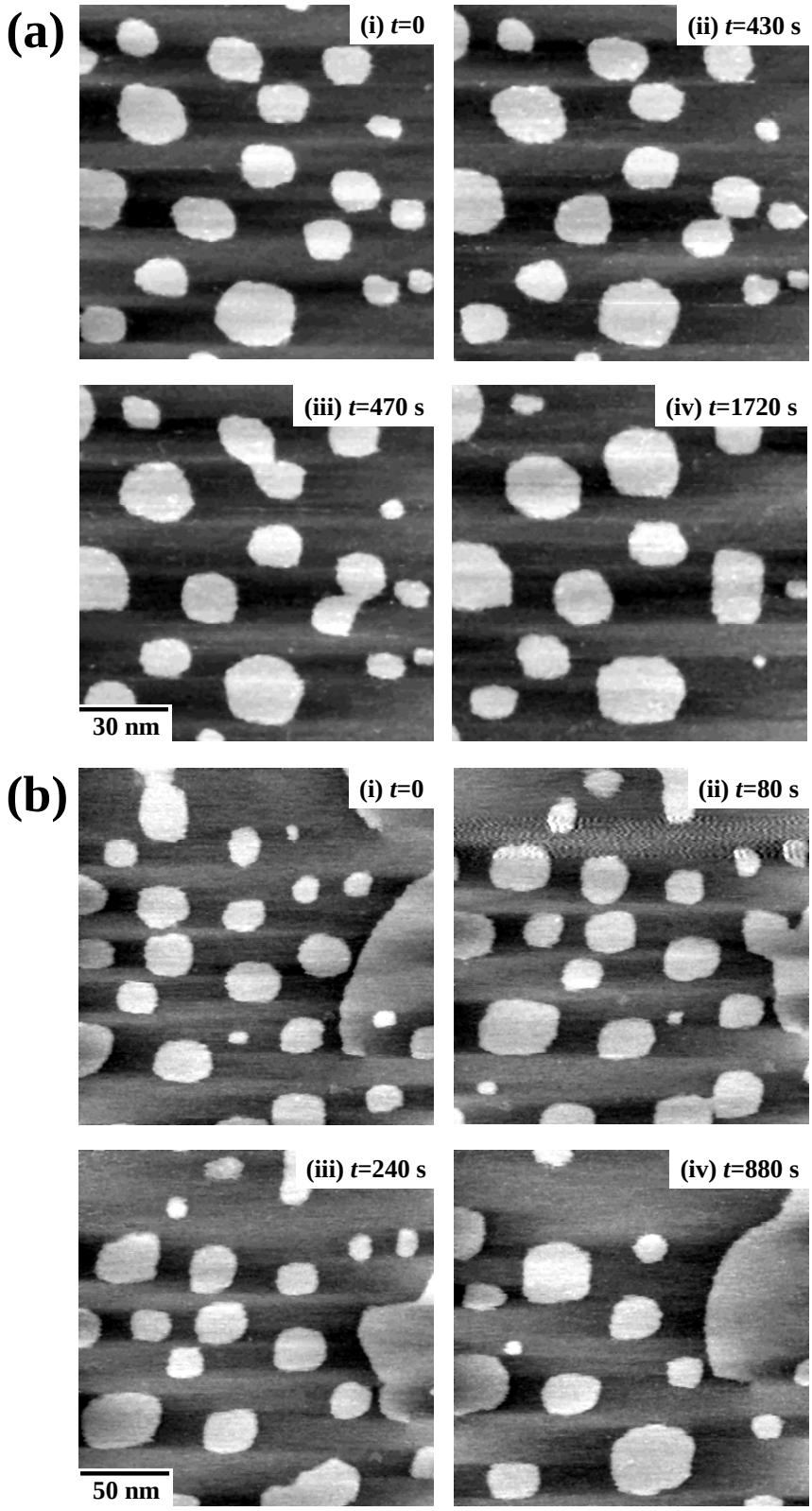
(a)
(i) t=0
(ii) t=430 s
(iii) t=470 s
(iv) t=1720 s
30 nm
(b)
(i) t=0
(ii) t=80 s
(iii) t=240 s
(iv) t=880 s
50 nm

Fig. 2

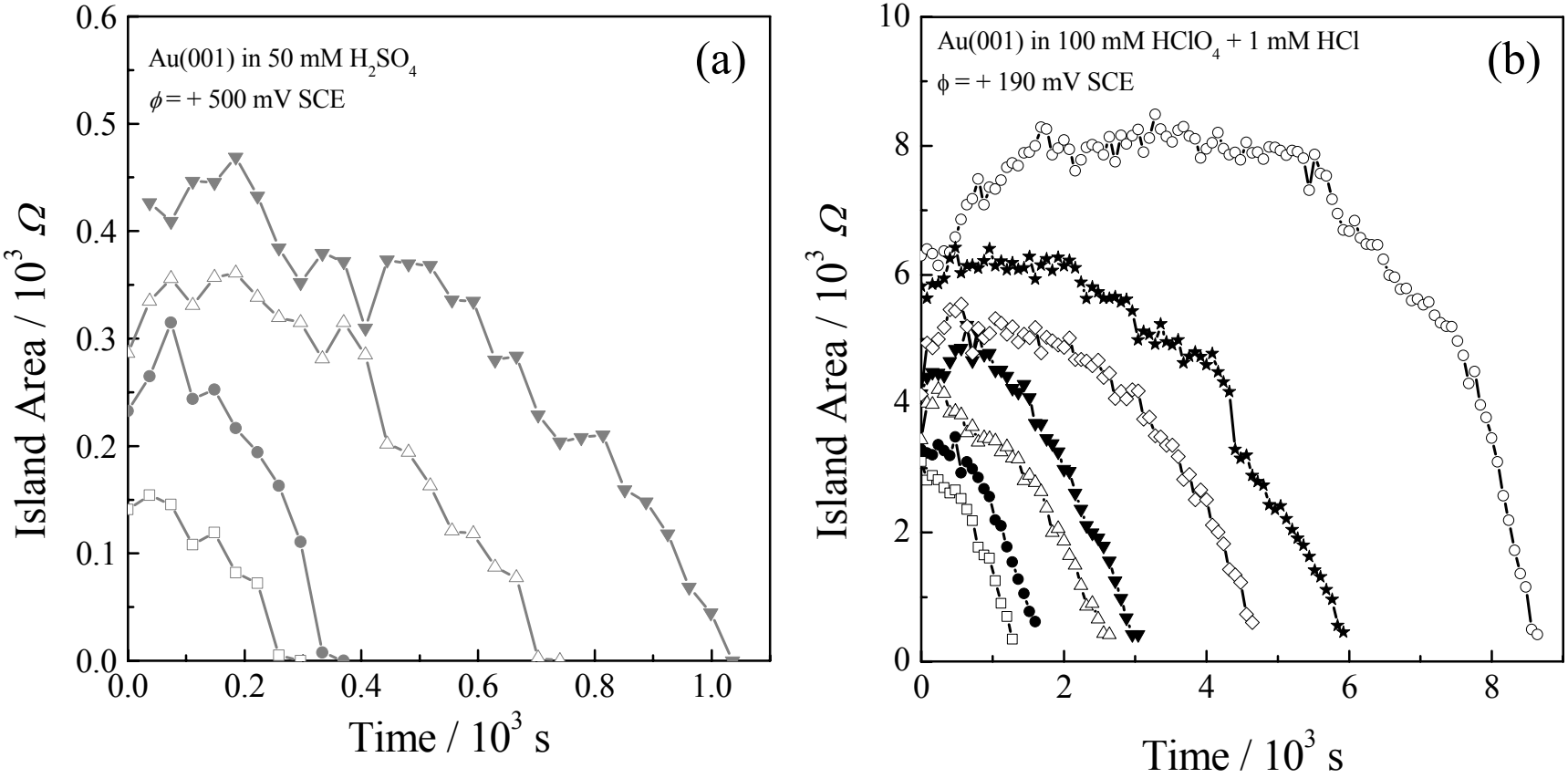
Au(001) in 50 mM H_2SO_4
ϕ = + 500 mV SCE
(a)
Island Area / 10^3 Ω
Time / 10^3 s
0.0
0.1
0.2
0.3
0.4
0.5
0.6
0.0
0.2
0.4
0.6
0.8
1.0
Au(001) in 100 mM $HClO_4$ + 1 mM HCl
ϕ = + 190 mV SCE
(b)
Island Area / 10^3 Ω
Time / 10^3 s
0
2
4
6
8
10
0
2
4
6
8

Fig. 3

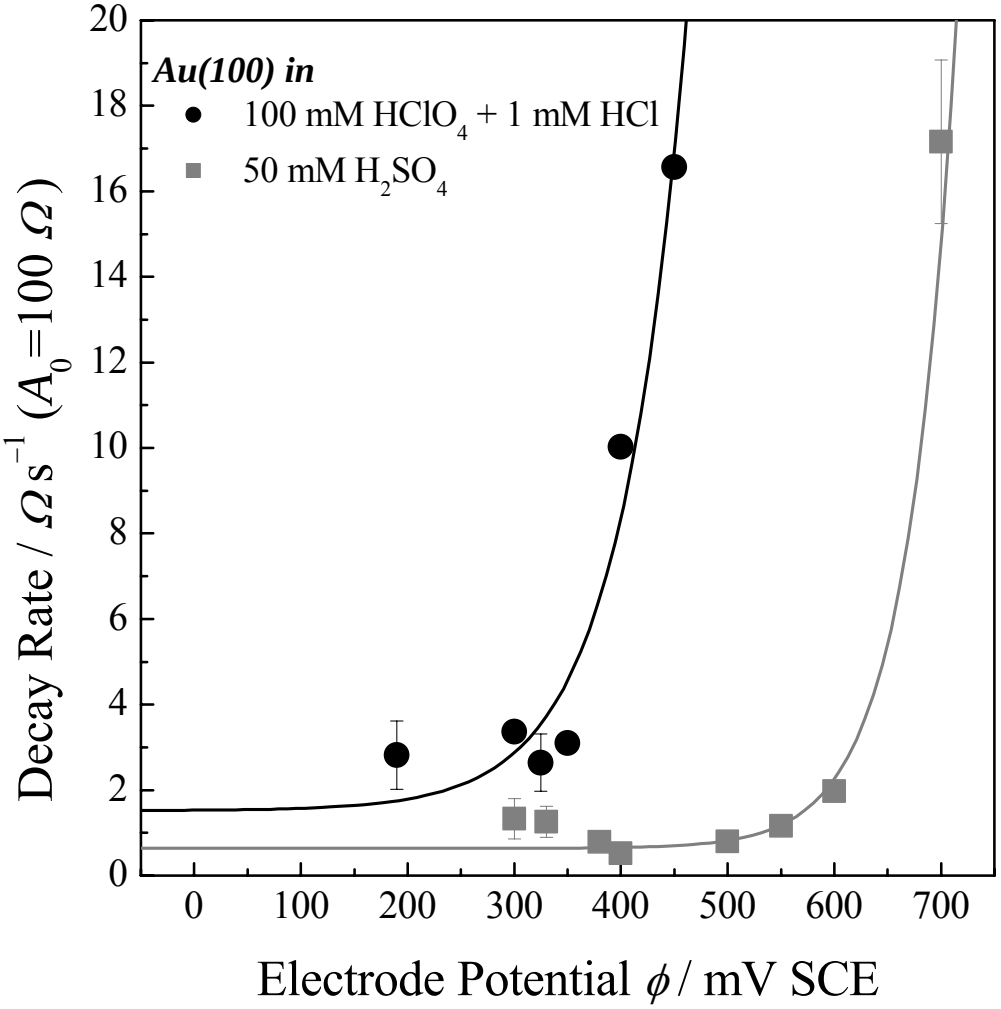
Au(100) in
100 mM HClO4 + 1 mM HCl
50 mM H2SO4
Decay Rate / Ω s−1 (A0=100 Ω)
Electrode Potential φ / mV SCE
0
2
4
6
8
10
12
14
16
18
20
0
100
200
300
400
500
600
700

Fig. 4

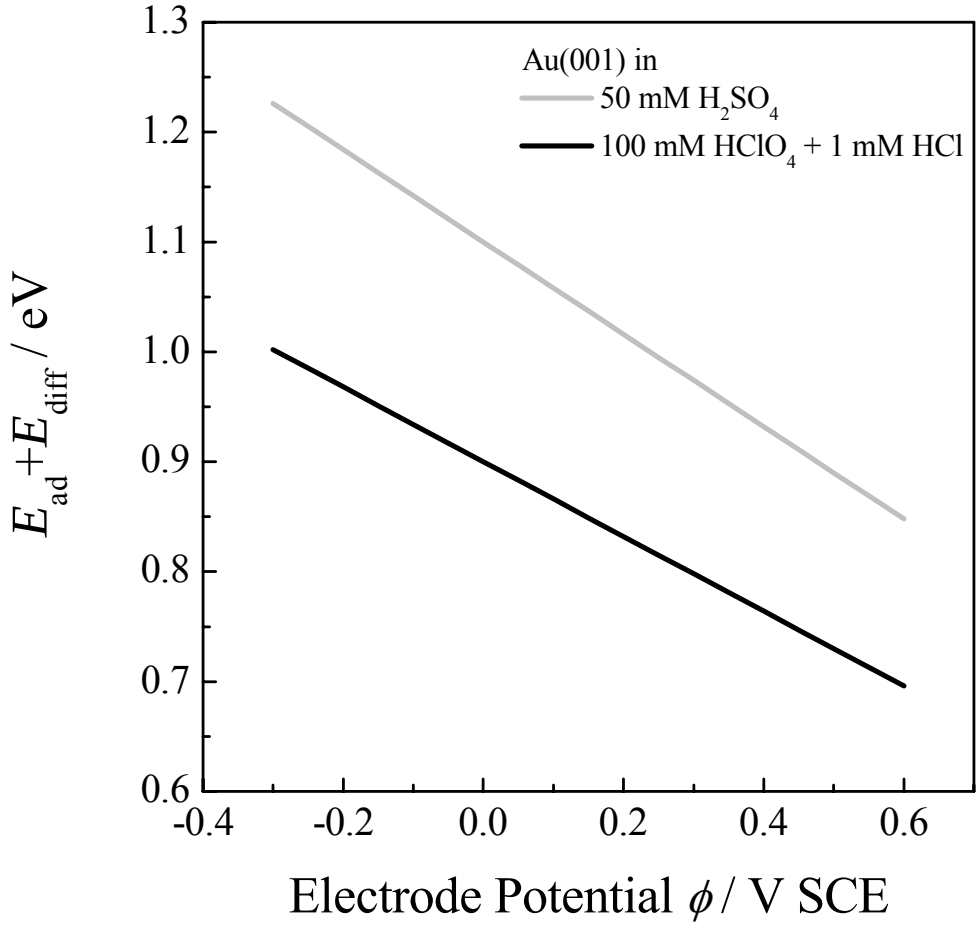
Au(001) in
50 mM H_2SO_4
100 mM $HClO_4$ + 1 mM HCl
$E_{ad}+E_{diff}$ / eV
1.3
1.2
1.1
1.0
0.9
0.8
0.7
0.6
-0.4
-0.2
0.0
0.2
0.4
0.6
Electrode Potential ϕ / V SCE

Fig. 5

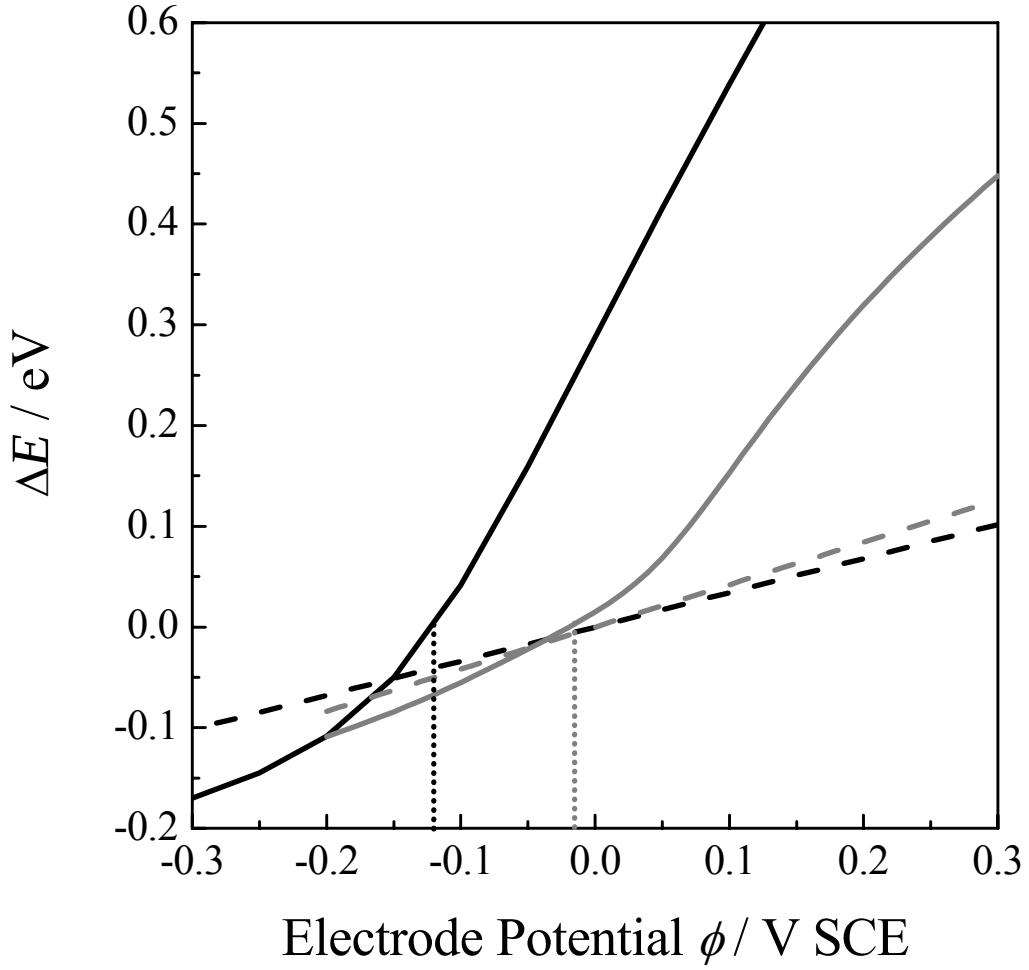
0.6
0.5
0.4
0.3
0.2
0.1
0.0
-0.1
-0.2
ΔE / eV
-0.3
-0.2
-0.1
0.0
0.1
0.2
0.3
Electrode Potential φ / V SCE

Fig. 6